AAPT PHYSICS EDUCATION | AMERICAN JOURNAL of PHYSICS

Exact solution of the compressed hydrogen atom

J. M. Ferreyra and C. R. Proetto

Citation: American Journal of Physics **81**, 860 (2013); doi: 10.1119/1.4820244
View online: http://dx.doi.org/10.1119/1.4820244
View Table of Contents: http://scitation.aip.org/content/aapt/journal/ajp/81/11?ver=pdfcov
Published by the American Association of Physics Teachers

Exact solution of the compressed hydrogen atom

J. M. Ferreyra[a)]
Departamento de Física, Facultad de Ciencias Exactas y Tecnología, Universidad Nacional de Tucumán, Av. Independencia 1800, (4000) S. M. de Tucumán, Argentina

C. R. Proetto[b)]
Centro Atómico Bariloche and Instituto Balseiro, 8400 S.C. de Bariloche, Río Negro, Argentina

(Received 8 March 2013; accepted 19 August 2013)

The exact solution to the problem of a hydrogen atom confined in a spherical well (CHA) is discussed; the standard results for the unconfined hydrogen atom (UHA) are recovered as the sphere size becomes large compared to the Bohr radius. The solutions are characterized by a set of three quantum numbers N (= 1, 2, 3,…), L (= 0, 1, 2,…), and M (= $-L$, $-L+1$,…, $L-1$, L), and the energy eigenvalues, in contrast to the situation in the UHA, depend on both N and L. All members of a given family $n=N+L$, however, evolve asymptotically toward the same energy level in the large-sphere limit, recovering the typical n^2 degeneracy of the UHA. Besides numerically exact solutions for arbitrary sphere sizes, rigorous analytical approximations are provided for the physically relevant strong- and weak-confinement regimes. A conjecture concerning the ordering of the energy levels is rigorously confirmed. The validity of the virial theorem, Kato's cusp condition, and the role played by the density as an alternative basic variable for the case of the CHA are discussed. © *2013 American Association of Physics Teachers.*
[http://dx.doi.org/10.1119/1.4820244]

I. INTRODUCTION

The quantum-mechanical problem of a hydrogen atom with the nucleus clamped at the center of a sphere of radius R, with infinite potential energy outside the sphere, was introduced by Michels *et al*. to model the effect of pressure on the states of hydrogen atoms in stars and gaseous planets.[1] The model was interesting enough to attract Sommerfeld's[2] attention and was further elaborated on by DeGroot *et al*.[3] More recently, the same model has been analyzed using a variety of perturbative and variational techniques.[4–11]

Besides its importance in atomic physics and astrophysics, the confined hydrogen atom (CHA) is relevant to bulk and nano-structured semiconductors (i.e., quantum dots), as according to the effective-mass theory of Luttinger and Kohn[12] the behavior of donor and acceptor impurities in a host semiconductor can be approximated by an extra charge (electron or hole) orbiting around the ionized parent impurity. This hydrogen-atom type of model (with some refinements related to details of the band structure of the host semiconductor) forms the basis of our present understanding of shallow impurities in bulk and confined semiconductors.[13,14,30] The physics of the CHA may be also useful as a simple model of ionized plasma properties[15,16] and for atoms encapsulated in fullerene.[17]

We provide here numerical and limiting analytical exact results for the CHA, using the rigorous mapping of its radial Schrödinger equation with the second-order differential equation satisfied by the so-called Kummer functions (Ref. 18, p. 504). While this approach has been already used for the calculation of some selected electronic states,[19–22] here, we extend this approach to essentially the full relevant spectrum of the CHA. With these results at hand, we obtain more complete insight on the CHA electronic spectrum and its dependence on pressure or confining sphere size. The main results are as follows: (i) the issue of the quantum numbers and the ordering of the energy levels of the CHA have been clarified; (ii) the size dependence of the lowest electronic states of the CHA has been found numerically and displayed in Fig. 1; (iii) rigorous analytical approximations have been derived in the physically relevant limits of weak and strong confinement; and (iv) the application of a modified version of the virial theorem, valid for confined systems, has been exemplified, together with a discussion of Kato's cusp condition and the essential role played by the electronic density alone as an alternative basic variable.

II. EXACT SOLUTION IN TERMS OF KUMMER FUNCTIONS

Owing to the wide disparity of the nuclear and electron masses, we start by writing the Schrödinger equation for an electron in the field of a nucleus of charge Ze and infinite mass, both confined within a sphere of radius R, with the nucleus located at the center of the sphere:

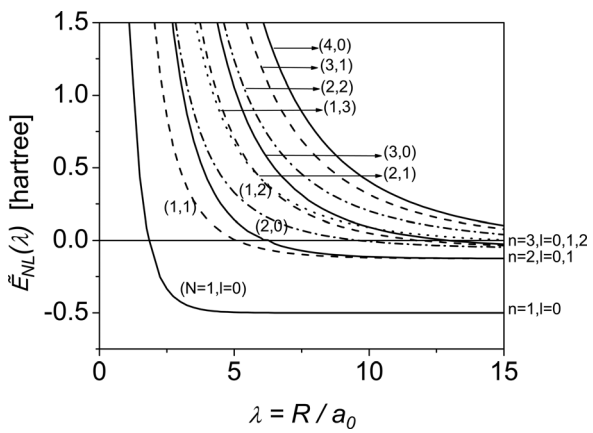

Fig. 1. Eigenenergies of the compressed hydrogen atom as a function of the atom size, for the four lowest-lying families corresponding to $N+L=1$, 2, 3, 4. To leading order, the asymptotic limits for $\tilde{E}_{NL}(\lambda)$ are $a_{NL}^2/(2\lambda^2)$ for $\lambda \to 0$, and $-1/[2(N+L)^2]$ for $\lambda \gg 1$ (see text). The asymptotic values for $\lambda \gg 1$ are $-1/2$, $-1/8$, $-1/18$, and $-1/32$.

$$[\hat{T}+\hat{V}]\Psi(\mathbf{r})=\left[-\frac{\hbar^2}{2m}\nabla^2-\frac{Ze^2}{r}\right]\Psi(\mathbf{r})=E\Psi(\mathbf{r}). \quad (1)$$

Here $\hat{T}$ and $\hat{V}$ are the kinetic- and potential-energy operators, respectively. The boundary conditions on $\Psi(\mathbf{r})$ are that it must remain finite at $r=0$ and that $\Psi(R)=0$ (hard-wall boundary condition). This last condition distinguishes the CHA from the standard unconfined hydrogen atom (UHA), where one imposes the requirement that the eigenfunction be bounded at infinity.[23]

Both the Coulomb and confining potentials are spherically symmetric, so Eq. (1) can be separated in spherical polar coordinates. Let r, θ, and ϕ be the coordinates of the electron. Proposing a separable solution of the type $\Psi(\mathbf{r})=[u(r)/r]Y_L^M(\theta,\phi)$ (Y_L^M being the spherical harmonic identified by the usual angular momentum quantum numbers $L=0, 1, 2,\ldots$ and $M=-L, -L+1,\ldots, L-1, L$), we arrive at the well-known differential equation for the radial functions

$$\left[\frac{1}{2}\frac{d^2}{d\tilde{r}^2}+\frac{Z}{\tilde{r}}-\frac{L(L+1)}{2\tilde{r}^2}+\tilde{E}\right]u(\tilde{r})=0, \quad (2)$$

written in terms of dimensionless variables $\tilde{r}=r/a_0$ and $\tilde{E}=E/\mathrm{Ha}$, where $a_0=\hbar^2/me^2$ and $\mathrm{Ha}=e^2/a_0=me^4/\hbar^2$. (For semiconductors in the effective mass framework, we would replace $e^2\to e^2/\varepsilon$ and $m\to m^*$, ε and m^* being the static dielectric constant and effective electron mass, respectively, for the host semiconductor.)

Finally, defining $\rho=2Z\tilde{r}/\alpha$, with $\alpha=\sqrt{-Z^2/2\tilde{E}}$ (assuming that $\tilde{E}<0$), and $u(\tilde{r})=u(\rho)=e^{-\rho/2}\rho^{1+L}w(\rho)$, we obtain

$$\left[\frac{d^2}{d\rho^2}+\left(-1+\frac{2+2L}{\rho}\right)\frac{d}{d\rho}-\frac{1+L-\alpha}{\rho}\right]w(\rho)=0, \quad (3)$$

whose two independent solutions are the regular $M(a,b,\rho)$ and irregular $U(a,b,\rho)$ confluent hypergeometric or Kummer functions, with $a=1+L-\alpha$, $b=2+2L$ (Ref. 18, p. 504). Because the irregular solution $U(1+L-\alpha,2+2L,\rho)\to\Gamma(1+2L)/\Gamma(1+L-\alpha)\rho^{-(1+L)}$ as $\rho\to 0$, $u(\rho)$ remains finite at the origin, but $\Psi(\mathbf{r})$ diverges as r^{-1} when $r\to 0$. In other words, $U(1+L-\alpha,2+2L,\rho)$ is not a permissible solution of Eq. (3) as it leads to an unphysical eigenfunction; accordingly, the (unnormalized) eigenfunction is simply $w(\rho)=M(a,b,\rho)$.

Imposing the hard-wall boundary condition $w(2ZR/\alpha a_0)=0$, we obtain the eigenvalue equation for negative energies

$$M(1+L-\alpha,2+2L,2ZR/\alpha a_0)=0. \quad (4)$$

What happens if $\tilde{E}>0$? The quantity α is now purely imaginary: $\alpha=-i\sqrt{Z^2/2\tilde{E}}=i\beta$ (β real and negative) and consequently the eigenvalue equation becomes $M(1+L-i\beta,2+2L,-2iZR/\beta a_0)=0$. However, to avoid the cumbersome task of working with complex magnitudes, it is convenient to exploit the following equivalence between the confluent hypergeometric and Coulomb functions (Ref. 18, p. 538):

$$F_L(\eta,\rho)=C_L(\eta)\rho^{1+L}e^{-i\rho}M(1+L-i\eta,2+2L,2i\rho), \quad (5)$$

with $C_L(\eta)=2^Le^{-\pi\eta/2}|\Gamma(1+L+i\eta)|/\Gamma(2+2L)$.

From Eq. (5), it is clear that the eigenvalue equation for positive $\tilde{E}$ is

$$F_L(\beta,-ZR/\beta a_0)=0, \quad (6)$$

where $\beta<0$ and $\beta^2=Z^2/2\tilde{E}$. Equations (4) and (6) provide the exact energies $\tilde{E}_{NL}(R/a_0)$ of the CHA. We will proceed now with their numerical and analytical (in limiting cases) analysis. From here on, we set $Z=1$.

III. NUMERICAL AND ANALYTICAL RESULTS

The numerical solution of Eqs. (4) and (6) yields the lowest-lying eigenenergies $\tilde{E}_{NL}(R/a_0)$ of the compressed hydrogen atom displayed in Fig. 1, as a function of the size R. Each energy level is characterized (in principle) by a set of three quantum numbers: N, L, M. As in the case of the UHA, the energy levels are independent of M; this independence has its origin in the fact that all directions in space enter on equal terms and leads to a degeneracy of $2L+1$ for each (N, L) pair. An important difference with respect to the UHA is that the energy levels of the CHA *do* depend on the quantum number L: the so-called "accidental degeneracy" of the UHA is a special property of the exact Coulomb potential Z/r, which is lifted when one adds the confining potential.

The quantum number N is a radial quantum number that enumerates the different solutions of Eqs. (4) and (6) corresponding to the same set of R and L values. For example, $N=1$ denotes the lowest-energy solution corresponding to a given L (the absolute ground-state corresponding to $N=1$, $L=0$); $N=2$ denotes the next-lowest-energy state for the same L; and so on. In the limit $\lambda=R/a_0\gg 1$, the solutions of the UHA with quantum numbers n, l, m and energies $-1/(2n^2)$ are recovered, as expected. More to the point, $\tilde{E}_{N,L}(\lambda\to\infty)\to -1/[2(N+L)^2]$ and $M(1+L-\alpha,2+2L,\rho)\to M(1+L-n,2+2L,\rho)\sim L_{n-1-L}^{2L+1}(\rho)$, with $L_n^{(\alpha)}(x)$ the generalized Laguerre polynomials, which are the well-known exact radial eigenfunctions of the UHA.[24]

Based on these results, the following equivalence can be established between the CHA and the UHA quantum numbers: as $\lambda\to\infty$, $N+L\to n$ and $L\to l$, while $M=m$ for all λ.

It is instructive to calculate the number of radial nodes to the UHA quantum numbers in the $R\to\infty$ limit. For any R, we known that the number of radial nodes is $N-1$. As $\lambda=R/a_0\to\infty$, $N-1\to n-L-1\to n-l-1$, which is the well-known counting of radial nodes of the UHA. One can easily check than the number of members for each "family" $N+L=n$ of the CHA is equal to n^2, the degeneracy associated with each energy level of the UHA. Within a given family, and for any finite λ, the eigenenergies obey the inequalities $\tilde{E}_{N=1,L=n-1}(\lambda)<\tilde{E}_{N=2,L=n-2}(\lambda)<\ldots<\tilde{E}_{N=n,L=0}(\lambda)$.[25] This feature is easily explained by the fact that as N increases, the number of radial nodes also increases, so the state becomes more widely distributed inside the spherical well and consequently feels more the presence of the confinement barrier whose effect is always to increase the energy. It is important to note that no link exists between N and L in the CHA; in particular, as shown in Fig. 1, it is permissible to have states where L is equal to or greater than N.

The exact value of λ for which the energy $\tilde{E}$ changes sign can be determined from Eq. (4) or Eq. (6), by putting $\tilde{E}=0$ and solving for λ.[2] If we employ Eq. (4), as $\tilde{E}\to 0^-$, $\alpha\to\infty$, but the product of the first and third arguments of M remains

finite and equal to -2λ. This suggests that from the series expansion of M,

$$M(a,b,\rho) = 1 + \frac{a}{b}\frac{\rho}{1!} + \frac{a(a+1)}{b(b+1)}\frac{\rho^2}{2!} + \cdots, \tag{7}$$

as $a \to -\infty$ but $a\rho$ remains finite, one can approximate the series by retaining (only) terms like $(a\rho)^n$. Proceeding in this way, it is not difficult to prove that the zeros of Eq. (4) are given by the zeros of $J_{1+2L}(2\sqrt{2\lambda})$, with $J_\nu(z)$ the cylindrical Bessel function of order ν (Ref. 18, p. 358). For instance, the first zero of $J_1(z)$ $(L=0)$ corresponds to $z_1 \simeq 3.832 = 2\sqrt{2\lambda} \to \lambda \simeq 1.835$, in agreement with the results of Fig. 1. This property can be used to determine, without any calculation, the number of "bound" states for a given size λ: it is enough to count the number of zeros of cylindrical Bessel functions smaller than $z_{\max} = 2\sqrt{2\lambda}$.

Next let us analyze the strong-confinement limit of small sizes $(\lambda \to 0)$ and the opposite limit of weak confinement corresponding to the large sizes $(\lambda \to \infty)$, where analytical results are available.

In the strong-confinement approximation (SCA), we consider the Coulomb interaction, which goes like $1/\lambda$, to be a small perturbation to the confinement effect (kinetic energy) which goes like $1/\lambda^2$ in the $\lambda \to 0$ limit.[26] To prove this, it will be convenient to express the Coulomb wavefunction as (Ref. 18, p. 540)

$$F_L(\beta, -\lambda/\beta) = -(1+2L)!!\,\frac{\lambda}{\beta}\,C_L(\beta)\sum_{k=L}^{\infty} b_k\, j_k(-\lambda/\beta), \tag{8}$$

where $(1+2L)!! = 1\cdot 3\cdot 5\cdots(1+2L)$, $j_k(\rho) = (\pi/2\rho)^{1/2} J_{k+1/2}(\rho)$ are the spherical Bessel functions, $b_L = 1$, $b_{L+1} = [(3+2L)/(L+1)]\beta$, and

$$b_k = c_k \times \left[2\beta b_{k-1} - \frac{(k-1)(k-2) - L(L+1)}{2k-3} b_{k-2}\right], \tag{9}$$

for $k > L+1$, $c_k = (2k+1)/[k(k+1) - L(L+1)]$. As $\lambda \to 0$, $\tilde{E} \to \infty$, and consequently $\beta \to 0$, we can simplify Eq. (8) in this limit by keeping the leading terms in powers of β. Proceeding in this way, we obtain

$$F_L\left(\beta \to 0, \frac{-\lambda}{\beta}\right) \sim j_L\left(\frac{-\lambda}{\beta}\right) + 2\beta\sum_{k=0}^{\infty}(-1)^k c_{k'}\, j_{k'}\left(\frac{-\lambda}{\beta}\right), \tag{10}$$

where $k' = 2k + L + 1$.[27] The eigenvalue equation is, as always, $F_L(\beta \to 0, -\lambda/\beta) = 0$.

To order β^0, the eigenvalue equation reduces to $j_L(-\lambda/\beta) = 0$, whose solutions are $-\lambda/\beta = a_{NL}$, with a_{NL} the Nth zero of the spherical Bessel function of order L. To this order, we obtain for the eigenvalue $1/(2\beta^2) = \tilde{E}_{NL}(\lambda) \simeq a_{NL}^2/(2\lambda^2)$; that is, we recover the characteristic R^{-2} dependence for the energy levels of a particle confined in a spherical box, as a consequence of the confinement-induced increase of the kinetic energy.[26]

The presence of the nucleus is apparent at the next order in β: assuming a solution of the type $-\lambda/\beta \simeq \rho_0 + \rho_1 = a_{NL} + \rho_1 (\rho_1 \ll a_{NL})$ and expanding Eq. (10) around a_{NL}, we obtain an equation for ρ_1, whose solution is $\rho_1 = \beta f_L(a_{NL})$, where

$$f_L(a_{NL}) = -\frac{2}{j'_L(a_{NL})}\sum_{k=0}^{\infty}(-1)^k c_{k'}\, j_{k'}(a_{NL}). \tag{11}$$

The eigenvalue equation (correct to order β) is $-\lambda/\beta = a_{NL} + \beta f_L(a_{NL})$, whose solution is

$$\frac{1}{2\beta^2} = \tilde{E}_{NL}(\lambda) \simeq \frac{1}{2}\left(\frac{a_{NL}}{\lambda}\right)^2 - \frac{f_L(a_{NL})}{\lambda}. \tag{12}$$

The whole physics of the CHA in the small-size limit is contained in this equation: while the term that goes like λ^{-2} reflects the effect of the confinement on the electron kinetic energy, the term proportional to λ^{-1} results from the effect of confinement on the Coulomb interaction.

The case $L=0$ turns out to be particularly simple: $x_{N0} = N\pi$, and

$$f_0(x_{N0}) = 3 + \frac{7}{6}\left[1 - \frac{15}{(N\pi)^2}\right] + \frac{11}{15}\left[1 - \frac{105}{(N\pi)^2} + \frac{945}{(N\pi)^4}\right] + \cdots. \tag{13}$$

For $N=1$, $f_0(x_{10}) \simeq 2.439$, which compares quite well with the "exact" result obtained from first-order perturbation theory where $f_0(x_{10}) = \mathrm{Cin}(2\pi) \simeq 2.438$.[28]

The exact numerical results of Fig. 1 are compared with the SCA just discussed in Fig. 2 and Table I. The SCA is an excellent approximation throughout the shaded upper region of the figure. This region is defined by the criterion that the SCA should be valid when the size R is smaller than the characteristic atom size. Using the average distance of the electron from the nucleus of the UHA[29,30] to quantify this atom size, we obtain $1.5a_0$ for the $1s$ state; $6a_0$ and $5a_0$ for the $2s$ and $2p$ states, respectively; $13.5a_0$, $12.5a_0$, and $10.5a_0$

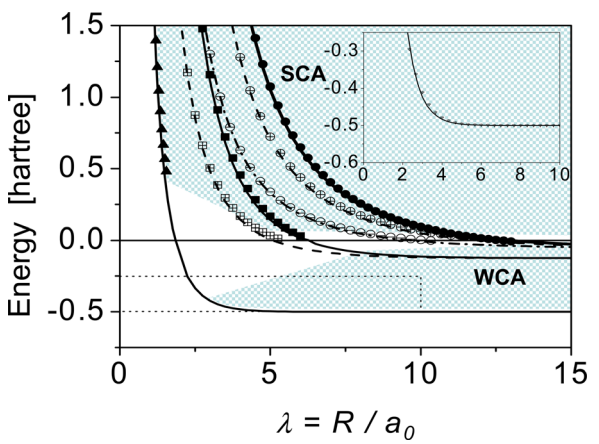

Fig. 2. Comparison of the exact eigenvalues of Fig. 1 (lines) with those obtained from the strong- and weak-confinement approximations (discrete points). The inset (corresponding to the rectangle marked at the lower left corner of the figure) shows the accuracy of the weak-confinement approximation given by Eq. (13), as applied to the ground state. The shaded upper and lower areas represent the regions of applicability of the SCA and the WCA, respectively.

Table I. Numerical values of $\tilde{E}_{NL}(\lambda)$, for the six lowest-lying electronic levels of the CHA, in Hartree units. For each λ, the first row (numbers in bold) corresponds to the exact (numerical) solution of Eq. (4) ($\tilde{E}_{NL}(\lambda) < 0$), or Eq. (6) ($\tilde{E}_{NL}(\lambda) > 0$). The second and third rows correspond to the SCA as given by Eq. (12), and as given by the zero-order approximation $\tilde{E}_{NL}(\lambda) \simeq a_{NL}^2/(2\lambda^2)$, respectively. For the ground state (1,0), the results of the WCA as given by Eq. (16) have also been included (numbers in italics).

$\lambda\,[R/a_0]$	(1,0)	(1,1)	(2,0)	(1,2)	(2,1)	(3,0)
0.50	**14.748**	**36.659**	**72.672**	**63.160**	**114.643**	**170.585**
	14.864	36.671	72.728	63.156	114.651	170.620
	19.739	40.374	78.957	66.424	119.351	177.653
1.00	**2.374**	**8.223**	**16.570**	**14.967**	**27.474**	**40.863**
	2.497	8.242	16.625	14.972	27.487	40.897
	4.935	10.093	19.739	16.606	29.838	44.413
1.50	**0.437**	**3.231**	**6.644**	**6.285**	**11.679**	**17.362**
	0.568	3.252	6.696	6.291	11.694	17.395
	2.193	4.486	8.773	7.380	13.261	19.739
	−0.052					
2.00	**−0.125**	**1.576**	**3.327**	**3.327**	**6.269**	**9.314**
	−0.207	1.597	3.377	3.334	6.284	9.345
		2.523	4.935	4.152	7.459	11.103
2.50	**−0.335**	**0.852**	**1.865**	**1.996**	**3.818**	**5.670**
	−0.332	0.874	1.912	2.003	3.834	5.700
		1.614	3.158	2.657	4.774	7.106
3.00	**−0.424**	**0.481**	**1.112**	**1.293**	**2.516**	**3.735**
	−0.411	0.504	1.155	1.300	2.532	3.763
		1.121	2.193	1.845	3.315	4.935
3.50	**−0.464**	**0.271**	**0.682**	**0.881**	**1.748**	**2.595**
	−0.455	0.295	0.721	0.889	1.764	2.621
		0.824	1.611	1.356	2.436	3.626
4.00	**−0.483**	**0.143**	**0.420**	**0.621**	**1.261**	**1.873**
	−0.479	0.168	0.455	0.629	1.277	1.897
		0.631	1.233	1.038	1.865	2.776
4.50	**−0.492**	**0.062**	**0.252**	**0.449**	**0.935**	**1.389**
	−0.490	0.087	0.282	0.457	0.951	1.412
		0.498	0.975	0.820	1.473	2.193
5.00	**−0.496**	**0.004**	**0.141**	**0.329**	**0.708**	**1.053**
	−0.495		0.166	0.337	0.723	1.073
			0.789	0.664	1.194	1.777
5.50	**−0.498**	**−0.029**	**0.064**	**0.243**	**0.543**	**0.811**
	−0.497		0.086	0.252	0.559	0.829
			0.652	0.549	0.986	1.468
6.00	**−0.499**	**−0.055**	**0.015**	**0.180**	**0.421**	**0.632**
	−0.498		0.029	0.189	0.437	0.648
			0.548	0.461	0.829	1.234
6.50	**−0.500**	**−0.074**	**−0.024**	**0.133**	**0.329**	**0.495**
	−0.500			0.142	0.345	0.510
				0.393	0.706	1.051
7.00	**−0.500**	**−0.087**	**−0.051**	**0.097**	**0.258**	**0.397**
	−0.500			0.105	0.273	0.404
				0.339	0.609	0.906
7.50	**−0.500**	**−0.097**	**−0.071**	**0.068**	**0.202**	**0.314**
	−0.500			0.077	0.217	0.321
				0.295	0.530	0.790
8.00	**−0.500**	**−0.104**	**−0.085**	**0.046**	**0.157**	**0.246**
	−0.500			0.055	0.172	0.254
				0.259	0.466	0.694
8.50	**−0.500**	**−0.110**	**−0.095**	**0.028**	**0.122**	**0.195**
	−0.500			0.038	0.136	0.201
				0.230	0.413	0.615
9.00	**−0.500**	**−0.114**	**−0.103**	**0.014**	**0.092**	**0.153**
	−0.500			0.023	0.107	0.158
				0.205	0.368	0.548
9.50	**−0.500**	**−0.117**	**−0.108**	**0.002**	**0.069**	**0.118**
	−0.500				0.083	0.122
					0.331	0.492
10.00	**−0.500**	**−0.119**	**−0.113**	**−0.007**	**0.049**	**0.091**
	−0.500				0.063	0.092
					0.298	0.444

for the $3s$, $3p$, and $3d$ states, respectively; and so on. The preceding analysis can be stated in a slightly different form: for a fixed size R, the SCA works better as one moves to increasingly excited states. The explanation is quite simple—for a given size, higher-energy states (due to their larger extension) feel more the spherical boundary than the lower-energy states, and consequently the accuracy of the SCA improves.

An interesting feature of the SCA, displayed in Table I, is the relevance of the first-order correction in Eq. (12), even for the smallest sizes analyzed. The size of the correction runs from about 4% for the (3,0) CHA electronic level at $\lambda = 0.5$, to about 400% for the same state at $\lambda = 10$. Clearly, both contributions to Eq. (12) are absolutely needed for a semi-quantitative description of the CHA electronic levels, in their region of applicability. In the context of semiconductor quantum dots, the remarkable success of the SCA applied to the problem of a centered impurity as displayed in Fig. 2 gives a solid basis to the application of the same approximation to the problem of an arbitrarily located (off-centered) impurity, for which no exact solution is available.[28]

Next, we turn to the weak-confinement approximation (WCA). We use the following analytical strategy to analyze this regime. First, we note that since $\tilde{E} \to -1/(2n^2)$ when $\lambda \to \infty$, $\alpha^2 = -1/(2\tilde{E}) \to n^2$ in the same limit. That means that the first argument of M in the eigenvalue Eq. (4) approaches asymptotically the value $1+L-n$; for the particular case $n = 1+L$, the argument becomes arbitrarily small as $\lambda \to \infty$. We exploit this feature to simplify the series expansion of Eq. (7), keeping just linear terms in the small parameter $a \to 1+L-n$. Under these conditions, Eq. (7) can be approximated by

$$M(a \to 0, b, \rho \to \infty) \to 1 + a\,\Gamma(b)\,\frac{e^{\rho}}{\rho^{b}}, \tag{14}$$

using the asymptotic expansion $M(a,b,\rho \to \infty) \to \Gamma(b) e^{\rho} \rho^{a-b}/\Gamma(a)$ of the hypergeometric function. Solving the eigenvalue equation $M(a \to 0, b, \rho \to \infty) = 0$ for $\Delta\tilde{E}_{1L}(\lambda)$, with $\tilde{E}_{1L}(\lambda) = -1/[2(1+L)^2] + \Delta\tilde{E}_{1L}(\lambda)$, one obtains in a few steps the result $\Delta\tilde{E}_{1L}(\lambda) = A_{1L}\lambda^{2(1+L)}\ e^{-2\lambda/(1+L)}$, with the coefficient A_{1L} being defined below Eq. (16). All the remaining $n \neq 1+L$ cases can be treated similarly by using the recurrence relations of the hypergeometric function. For example, the case $a = 1+L-\alpha$, with $\alpha \to n = 2+L$, can be treated by using the exact recurrence relation (Ref. 18, p. 506)

$$M(a,b,\rho) = M(a+1,b,\rho) - \frac{\rho}{b} M(a+1,b+1,\rho). \tag{15}$$

Taking the asymptotic limit of this equation and considering now that the first argument of the M's on the right-hand side

is such that $a+1=2+L-\alpha \to 0$, one can continue as explained below Eq. (14).

Proceeding in this way, we have obtained the following general result in the limit $\lambda \to \infty$:

$$\tilde{E}_{NL}(\lambda) \simeq -\frac{1}{2(N+L)^2} + A_{NL}\,\lambda^{2(N+L)}\,e^{-2\lambda/(N+L)}, \qquad (16)$$

where $A_{NL} = 2^{2(N+L)}/[(N-1)!(2L+N)!(N+L)^{(3+2(N+L))}]$. In particular $\tilde{E}_{10}(\lambda) = -0.5 + 4\lambda^2 e^{-2\lambda}$, which coincides with the ground-state analysis of this regime in Refs. 8 and 31. The inset of Fig. 2 compares the WCA to the exact results.

Several features of this result are worth noting. First, the leading correction to the unconfined result $-1/[2(N+L)^2]$ is a non-analytical function of λ, which means that no series expansion in powers of the small parameter λ^{-1} exists in this regime. Physically, the exponentially small correction reflects the quite small effect that the hard-wall boundary exerts on the exponentially decaying hypergeometric radial functions. Second, all the members of a family $N+L=n$ have the same functional dependence on λ; they differ from each other only in the numerical factor A_{NL}.[32] And third, the result given by Eq. (16) is just the leading term, following (next-order) terms differing from the one written by having smaller powers of λ, and being consequently less important in the large-λ limit.

As a last interesting point, we note that all of the difference between the CHA and the UHA can be traced back to the difference in boundary conditions: hard-wall at the outer sphere in the first case, but bounded at infinity in the second case. This means that whenever one of the nodes of the radial eigenfunctions of the UHA coincides with the sphere boundary, the hard-wall boundary condition is automatically satisfied and the solutions of the CHA and UHA are equivalent (apart from a normalization factor that accounts for $\Psi^{\mathrm{CHA}}(R)=0$). A question remains, however, about how these special points are distributed among all possible solutions of the compressed hydrogen atom; we provide the answer in Fig. 3. Thus, the $2s$ state of the UHA with energy $-1/8=-0.125$ becomes the ground state $N=1, L=0$ of the CHA for the special size $\lambda=2$, where the unique $2s$ node and boundary coincide. As a general rule, when λ coincides with the first radial node of the nl state of the UHA, this hydrogenic function becomes the $N=1, L=l$ solution of the CHA; the second node is found related to the first-excited $N=2$ state for the same L, and so on. In the Appendix, we give some applications of these particular UHA solutions that are also solutions of the CHA for special values of R.

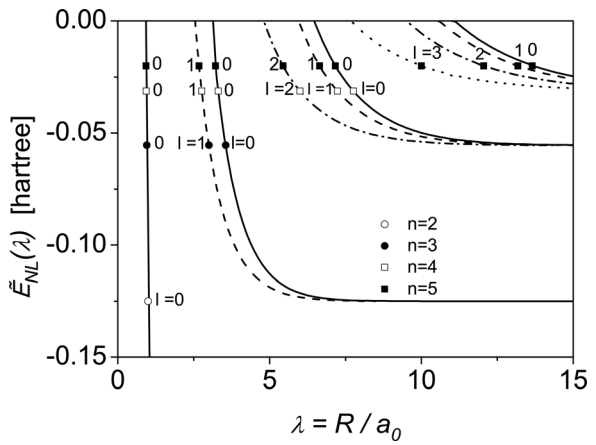

Fig. 3. Special sphere sizes (discrete points) for which certain CHA and UHA solutions coincide. Only the negative part of Fig. 1 is shown, following the same line convention. For example, the three black dots at $\tilde{E}_{NL}(\lambda) = -1/18 \sim -0.056$ correspond to the UHA solutions with $n=3, l=0$ (first node, at $\lambda = 3(6-\sqrt{12})/4 \sim 1.902$), $n=3, l=1$ (unique node, at $\lambda=6$), and $n=3, l=0$ (second node, at $\lambda = 3(6+\sqrt{12})/4 \sim 7.098$).

IV. CONCLUSIONS

In summary, we have fully analyzed the exact solution to the problem of a hydrogen atom confined in a spherical well. The standard unconfined three-dimensional solution becomes a limiting case of our solution, corresponding to the sphere boundary going to infinity. Based on our exact numerical results for the electronic spectra of the CHA, we have given a rigorous discussion of the quantum number issue and the ordering of the confined electronic levels. We have validated the physically relevant weak- and strong-confinement limits, where rigorous analytical approximations are available. The results presented here provide a rigorous basis for the important problem of doping with impurities of semiconductor heterostructures such as quantum dots.

ACKNOWLEDGMENTS

One of us (J.M.F.) is indebted to CONICET of Argentina for financial support at the starting stage of this project. C.R.P. is a fellow of CONICET. The authors thank J. Luzuriaga and V. H. Ponce for a careful reading of the manuscript.

APPENDIX: PARTICULAR UHA SOLUTIONS AS CHA SOLUTIONS

For all discrete points in Fig. 3, analytical expressions for the eigenstates of the CHA are available by exploiting the explicit expressions for the hydrogenic wavefunctions, as found in most textbooks on quantum mechanics.[24] For example, for $N=1$ and $L=M=0$, the exact solution of the confined hydrogenlike atom with $\lambda = 2/Z$ is given by

$$\Psi_{100}^{\mathrm{CHA}}(\tilde{r}) = \frac{\Psi_{2s}^{\mathrm{UHA}}(\tilde{r})}{\sqrt{1-7e^{-2}}} = \frac{1}{4\sqrt{2\pi}\sqrt{1-7e^{-2}}} Z^{3/2}(2-Z\tilde{r})e^{-Z\tilde{r}/2}, \qquad (A1)$$

with $0 \le \tilde{r} \le 2/Z$. Note the presence of the extra factor $\sqrt{1-7e^{-2}}$ in the denominator, which accounts for the difference between the extent of the radial normalization integral of the UHA ($[0,\infty]$), and the CHA with $\lambda = 2/Z$ ($[0, 2/Z]$). With these analytical expressions at hand, one can apply them to illustrate several concepts of the physics of the quantum mechanics of confined systems, as follows.

(a) Virial theorem for confined systems.[33] With the explicit expression in Eq. (A1), it is a standard exercise of quantum mechanics to check that $\langle\hat{T}\rangle + \langle\hat{V}\rangle = -Z^2/8$ as it should be. Here, $\langle\hat{T}\rangle = \langle\Psi_{100}^{\mathrm{CHA}}|\hat{T}|\Psi_{100}^{\mathrm{CHA}}\rangle = Z^2(1-3e^{-2})/[16(1-7e^{-2})]$ and $\langle\hat{V}\rangle = \langle\Psi_{100}^{\mathrm{CHA}}|\hat{V}|\Psi_{100}^{\mathrm{CHA}}\rangle = -Z^2(1-5e^{-2})/[8(1-7e^{-2})]$ are the kinetic- and potential-energy expectation values, evaluated with the state in Eq. (A1). Moreover, since

$$2\langle\hat{T}\rangle + \langle\hat{V}\rangle = \frac{1}{2}\frac{Z^2e^{-2}}{1-7e^{-2}}, \qquad (A2)$$

one finds that the usual expression for the quantum virial theorem, $2\langle\hat{T}\rangle + \langle\hat{V}\rangle = 0$, is only fulfilled up to exponential accuracy. On the other side, the result in Eq. (A2) nicely agrees with the result of the virial theorem for systems with boundaries, $2\langle\hat{T}\rangle + \langle\hat{V}\rangle = 3p\Omega$, with p being the pressure and Ω the volume of the confined system.[34] From Eq. (A2), one obtains $p(\lambda = 2/Z) = Z^5 e^{-2}/[64\pi(1 - 7e^{-2})]$. For $Z = 1$, this result was first obtained in Ref. 33.

(b) Kato cusp condition for confined systems. It has been long recognized that the many-electron wavefunction of any atom or molecule has a cusp at the nucleus position(s), which is a consequence of the singularity in the electron-nucleus Coulomb interaction, as the relative coordinate goes to zero. This exact condition on the many-electron wavefunction was first formulated in Ref. 35; it was later formulated in terms of the electronic density in Ref. 36. Because Kato's cusp condition usually refers to unconfined atoms and molecules, the question naturally arises about its validity for confined systems (like the CHA). The answer is again a didactic exercise of quantum mechanics: defining the density $n_{100}^{\mathrm{CHA}}(\tilde{r}) = \Psi_{100}^{\mathrm{CHA}}(\tilde{r})^2$, one can prove the following identity using Eq. (A1):

$$Z = -\frac{1}{2n_{100}^{\mathrm{CHA}}(\tilde{r})}\frac{dn_{100}^{\mathrm{CHA}}(\tilde{r})}{d\tilde{r}}\bigg|_{\tilde{r}\to 0}, \tag{A3}$$

which shows that Kato's cusp condition is also valid for confined systems, as expected.

(c) The electron density as a basic variable: elementary argument for confined systems. Equations (A1) and (A3) illustrate the far-reaching fact that a knowledge of the electron density is enough to determine the CHA Hamiltonian, by following the next steps: (i) integration of the density over all space yields the number of electrons (one in this case); (ii) from Kato's cusp condition [Eq. (A3)] one obtains the value of Z; (iii) from the position of the cusp ($\tilde{r} = 0$), one obtains the nucleus position; and (iv) since $n_{100}^{\mathrm{CHA}}(\tilde{r}) = 0$ if $\tilde{r} > 2/Z$, this determines the size of the CHA. With all this information one can "reconstruct" the Hamiltonian of the CHA as given in Eq. (1). Under much more general conditions, the same statement is essentially true for non-Coulombic potentials, but in this case only for the ground-state density. This is one of the basic pillars of the elaborated calculation scheme known as density functional theory, which is now the method of choice for the calculation of electronic properties in quantum chemistry and solid state physics.[37,38]

[a]Electronic mail: jferreyra64@gmail.com
[b]Electronic mail: mail:proetto@cab.cnea.gov.ar

[1]A. Michels, J. de Boer, and A. Bijl, "Remarks concerning molecular interactions and their influence on the polarizability," Physica (Amsterdam) **4**, 981–994 (1937).
[2]A. Sommerfeld and H. Welker, "Künstliche Grenzbedingungen beim Keplerproblem," Ann. Phys. (Leipzig) **424**, 56–65 (1938).
[3]S. R. DeGroot and C. A. Ten Seldam, "On the energy levels of a model of the compressed hydrogen atom," Physica **12**, 669–682 (1946).
[4]S. Yngve, "The compressed hydrogen atom," Am. J. Phys. **54**, 1103–1106 (1986).
[5]W. Wilcox, "A formula for energy displacements for the confined hydrogen atom," Am. J. Phys. **57**, 526–528 (1989).
[6]J. L. Marin and S. A. Cruz, "On the use of direct variational methods to study confined quantum systems," Am. J. Phys. **59**, 931–935 (1991).
[7]J. L. Marin, R. Rosas, and A. Uribe, "Analysis of asymmetric confined quantum systems by the direct variational method," Am. J. Phys. **63**, 460–463 (1995).
[8]D. Djajaputra and B. R. Cooper, "Hydrogen atom in a spherical well: Linear approximation," Eur. J. Phys. **21**, 261–267 (2000).
[9]M. L. Glasser and D. Bousquet, "Shooting for the stars: The spherically confined H-atom redux," Am. J. Phys. **71**, 574–576 (2003).
[10]F. M. Fernández, "The confined hydrogen atom with a moving nucleus," Eur. J. Phys. **31**, 285–290 (2010).
[11]H. E. Montgomery, Jr., "Variational perturbation treatment of the confined hydrogen atom," Eur. J. Phys. **32**, 1275–1284 (2011).
[12]J. M. Luttinger and W. Kohn, "Motion of electrons and holes in perturbed periodic fields," Phys. Rev. **97**, 869–883 (1955).
[13]W. Kohn, "Shallow impurity states in Silicon and Germanium," Solid State Phys. **5**, 257–320 (1957).
[14]G. Bastard, *Wave Mechanics Applied to Semiconductor Heterostructures* (Les Ulis, Les Editions de Physique, 1988).
[15]J. C. Stewart and K. D. Pyatt, Jr., "Lowering the ionization potentials in plasmas," Astrophys. J. **144**, 1203–1211 (1966).
[16]O. Ciricosta *et al.*, "Direct measurements of the ionization potential depression in a dense plasma," Phys. Rev. Lett. **109**, 065002 (2012).
[17]J.-P. Connerade, V. K. Dolmatov, and S. T. Manson, "A unique situation for an endohedral metallofullerene," J. Phys. B **32**, L395–L403 (1999).
[18]M. Abramowitz and I. A. Stegun, *Handbook of Mathematical Functions* (Dover, New York, 1970). The (free) online version of this book is at <http://dlmf.nist.gov>.
[19]S. Goldman and C. Joslin, "Spectroscopic properties of an isotropically compresed hydrogen atom," J. Phys. Chem. **96**, 6021–6027 (1992).
[20]S. H. Patil and Y. P. Varshni, "Properties of confined hydrogen and helium atoms," Adv. Quantum Chem. **57**, 1–24 (2009).
[21]B. L. Burrows and M. Cohen, "Exact solutions for confined model systems using kummer functions," Adv. Quantum Chem. **57**, 173–201 (2009).
[22]N. Aquino, G. Campoy, and H. E. Montgomery, Jr., "Highly accurate solutions for the confined hydrogen atom," Int. J. Quantum Chem. **107**, 1548–1558 (2007).
[23]Using a more precise mathematical terminology, the UHA wavefunction obeys a Neumann-type boundary condition, while the CHA wavefunction obeys a Dirichlet-type boundary condition.
[24]L. Pauling and E. B. Wilson, *Introduction to Quantum Mechanics* (McGraw-Hill, New York, 1935).
[25]This finding validates a conjecture formulated in Ref. 5, about the ordering of the CHA eigenvalues.
[26]L. Brus, "Electron-electron and electron-hole interactions in small semiconductor crystallites: The size dependence of the lowest excited electronic state," J. Chem. Phys. **80**(9), 4403–4409 (1984).
[27]In order to pass from Eq. (8) to Eq. (10), it is enough to calculate a few b_L values, using Eq. (9) and then keep only the linear contributions in β.
[28]J. M. Ferreyra and C. R. Proetto, "Strong confinement approach for impurities in quantum dots," Phys. Rev. B **52**, R2309–R2312 (1995); C. R. Proetto, "Comment on 'Screening in Semiconductor Nanocrystallites and its Consequences for Porous Silicon,'" Phys. Rev. Lett. **76**, 2824 (1996). Cin(x) refers to the Cosine integral function (Ref. 18, p. 231).
[29]Defined as $\bar{r}_{nlm} = \langle\Psi_{nlm}^{\mathrm{UHA}}|\mathbf{r}|\Psi_{nlm}^{\mathrm{UHA}}\rangle$. The explicit expression is $\bar{r}_{nlm} = n^2 a_0\{1 + [1 - l(l+1)/n^2]/2\}/Z$, as given in Ref. 24, p. 144.
[30]L. Bányai and S. W. Koch, *Semiconductor Quantum Dots* (World Scientific, Singapore, 1993).
[31]Y. Kayanuma, "Quantum-size effects of interacting electrons and holes in semiconductor microcrystals with spherical shapes," Phys. Rev. B **38**, 9797–9805 (1988).
[32]Within a given family, $n = N + \mathrm{L}$ and $A_{NL} = A_{N,n-N}$. Since $A_{N,n-N} < A_{N+1,n-N-1}$, this implies that $\tilde{E}_{N,n-N} < \tilde{E}_{N+1,n-N-1}$ [see Eq. (16)], in agreement with the discussion above on the ordering of the energy levels in Fig. 1.
[33]N. H. March and M. P. Tosi, "Caged H atom and H_2 molecule in relation to Monte Carlo study of molecular dissociation at constant volume", Il Nuovo Cimento D, **18**, 1061–1067 (1996).
[34]G. Marc and W. G. McMillan, "The virial theorem," Adv. Chem. Phys. **58**, 209–361 (1985).
[35]T. Kato, "On the eigenfunctions of many-particle systems in quantum mechanics," Commun. Pure Appl. Phys. **10**, 151–177 (1957).
[36]E. Steiner, "Charge densities in atoms," J. Chem. Phys. **39**, 2365–2366 (1963).
[37]R. G. Parr and W. Yang, *Density-Functional Theory of Atoms and Molecules* (Oxford U.P., New York, 1989).
[38]R. M. Dreizler and E. K. U. Gross, *Density Functional Theory* (Springer, Berlin, 1990).